International Journal of Mass Spectrometry 292 (2010) 38–47

Contents lists available at ScienceDirect

International Journal of Mass Spectrometry

journal homepage: www.elsevier.com/locate/ijms

ESI and MALDI mass spectrometry of large POSS oligomers

Stanley E. Anderson[b], Arpad Somogyi[c], Timothy S. Haddad[d], E. Bryan Coughlin[e], Gunjan Gadodia[e], David F. Marten[b], Julie Ray[b], Michael T. Bowers[a,*]

[a] Department of Chemistry & Biochemistry, University of California, Santa Barbara, CA 93106, United States
[b] Department of Chemistry, Westmont College, Santa Barbara, CA 93108, United States
[c] Department of Chemistry and Biochemistry, University of Arizona, Tucson, AZ 85721, United States
[d] ERC Inc., Air Force Research Laboratory, 10 East Saturn Boulevard, Building 8451, Edwards AFB, CA 93524-7680, United States
[e] Department of Polymer Science and Engineering, UMass, Amherst, MA 01003, United States

ARTICLE INFO

Article history:
Received 18 August 2009
Received in revised form 22 February 2010
Accepted 22 February 2010
Available online 1 March 2010

Keywords:
Polyhedral oligomeric silsesquioxane (POSS)
POSS
MALDI
Hybrid inorganic/organic

ABSTRACT

A series of Polyhedral Oligomeric Silsesquioxane (POSS) propylmethacrylate (PMA) and styryl oligomers were prepared from POSS monomers, $R_7R'Si_8O_{12}$, containing 1 functional R' group for polymerization and 7 inert R-groups where R = isobutyl (i-butyl), phenyl (Ph), cyclohexyl (Cy) or cyclopentyl (Cp). Both standard atom transfer radical polymerization (ATRP) and free radical syntheses, the latter employing azoisobutylnitrile as the free radical initiator were used in the syntheses. Matrix-assisted laser desorption ionization time-of-flight (MALDI-TOF) mass spectra were obtained in a new matrix, 4,4′-dihydroxyoctafluoroazobenzene which was especially designed for insoluble and intractable polymeric materials. Well-resolved series of oligomers were observed out to $n = \sim 13$ in both the linear and reflectron modes. Major peaks were assigned based on tandem mass spectrometry (MSMS) fragmentation patterns to give a consistent explanation of the observed spectra. In all cases, ionization of the ATRP products gave cationized parent ions in which the terminal Br atom was replaced by hydrogen. Additional observed peaks were due to loss of POSS side chains from the oligomer backbone. The free radical products were terminated with either one or two isobutylnitrile groups. Electrospray ionization (ESI) spectra were more complex than the MALDI-TOF but showed either identical parent ions or closely related hydroxylated parent ions.

1. Introduction

Polyhedral Oligomeric Silsesquioxanes (POSS) are a class of important hybrid inorganic/organic materials of the form $(RSiO_{3/2})_n$, or R_nT_n, where organic substituents are attached to a silicon-oxygen cage [1]. The most common and stable POSS cage is the T_8 (a molecule with a cubic array of silicon atoms bridged by oxygen atoms with an R group at each of the silicon vertices of the cube); other cages with well-defined geometries include $n = 6$, 10, 12, 14, 16 and 18 [2,3]. When these Si–O cages are introduced into organic polymers, new and useful materials are often realized [4–12] with enhanced properties superior to the original organic polymer. Current research on POSS materials has focused on developing new synthetic routes and creating POSS compounds with different cage sizes and organic substituents to obtain tailor-designed physical properties and allow the incorporation of POSS into a wide variety of polymer systems. Therefore, the goal of actually specifying structure–property relationships for these materials has important ramifications for significant applications.

The goal of our research collaboration has been to characterize the conformational preferences of various R_7T_8-POSS cages when coupled to oligomers in the $n = 2$–20 range and to determine conformer structures and isomer distributions of new materials using ion mobility mass spectrometry. The Bowers group has been successful so far in characterizing two oligomer systems, the POSS propylmethacrylates and siloxanes, but only up to species with three POSS cages [13,14] due to limitations in mass signal intensity.

There are to date only a few papers reporting mass spectra of POSS polymers and oligomers [15–23]. These studies all investigate systems, and especially synthetic intermediates, in which there are a large number of –OH groups. In our experience, the presence of such electronegative groups aids mass spectrometry by both matrix-assisted laser desorption ionization (MALDI) and electrospray ionization (ESI) because they facilitate cationization. This condition is seldom met for most POSS polymers and oligomers that do not have many electronegative groups. Another crucial condition for studying large POSS ions in the gas phase is absence of substantial fragmentation. While ion formation mechanisms in MALDI have been extensively reviewed, in general they are com-

* Corresponding author at: Department of Chemistry & Biochemistry, University of California, Santa Barbara, CA 93106, United States. Tel.: +1 805 893 2893.
E-mail address: bowers@chem.ucsb.edu (M.T. Bowers).

1387-3806/$ – see front matter © 2010 Elsevier B.V. All rights reserved.
doi:10.1016/j.ijms.2010.02.013

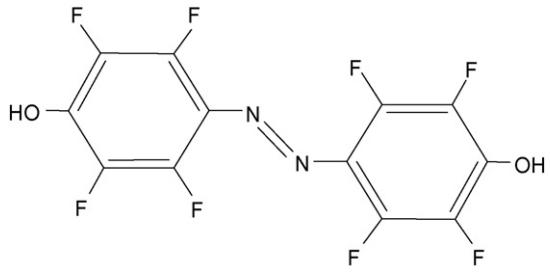

Fig. 1. 4,4′-Dihydroxyoctafluoroazobenzene matrix.

plicated and poorly understood [24,25]. Choice of an appropriate matrix is critical to obtaining mass spectra and really good matrices for POSS materials have been unavailable due to their insoluble and intractable nature.

Ion mobility mass spectrometry has been quite successful in studying large conventional polymers or biopolymers including DNA and peptides [26–32]. This methodology however is predicated on obtaining strong signals in the mass spectrum. Initial work with POSS materials using MALDI techniques [33,34] employed 2,5-dihydroxybenzoic acid (DHB) as a suitable matrix. The parent compounds are efficiently ionized due to electronegative atoms or localized π-electron density in the R-groups and readily bind protons or alkali metal cations to give abundant positive ions. Cage fragmentation does occur to some extent in all of these systems, especially at high laser power, but that did not prevent observation of strong molecular ion peaks for monomers and dimers. Trimers of mass ~3000 g/mol were more of a challenge, particularly to get enough intensity for ion mobility measurements. The nature of the cage R-group was found to be important. Bulky alkyl R-groups seem to inhibit the formation of positive ions and mass spectra for such POSS species are difficult to obtain. We hypothesize that larger POSS oligomers have lower ionization efficiencies than the monomers, most likely due to decreased charge density, since the POSS cages seem to be efficient in delocalizing electron density. Large systems also have an increased probability of fragmentation, e.g., loss of POSS side-chains.

For these reasons, the intensity of the "molecular ion" (in most cases sodiated or potassiated oligomer molecules) generally decreases with increasing oligomer size to the point that it becomes impossible to obtain ion mobility data. To facilitate the observation of higher POSS oligomers we have had to develop new strategies to enhance cationization (or anionization) efficiency. Certain POSS monomers [35,36] efficiently incorporate fluoride ion into the cage center to produce ionic species so we investigated fluoride as a structural probe. This proved successful only for POSS monomers containing R-groups which are electron-withdrawing or have delocalized π electron density. Fluoride also degrades POSS cages and ester linkages and, therefore, its incorporation into oligomers was not as successful a probe as we had hoped [37].

A remaining strategy is to find a better matrix for MALDI. Somogyi et al. have recently described a number of new matrices and especially the newly synthesized matrix 4,4′-dihydroxyoctofluoroazobenzene (see Fig. 1) [38]. It has proved successful for intractable polyester polymers such as Vectra and this suggests it might be suitable for large POSS oligomers. This matrix ostensibly works so well because the powerfully solvating tetrafluorophenolic group is incorporated directly into the matrix structure as well as the azobenzene functionality to impart appropriate UV-absorbing characteristics. We wish to report MALDI studies using this matrix on a number of representative POSS propylmethacrylate (PMA) and styryl systems that were difficult or even impossible to investigate using standard matrices.

2. Experimental

2.1. Synthesis of POSS compounds

2.1.1. Materials

Phthalic anhydride (99%+), 2-(2-aminoethoxy) ethanol (98%), N,N,N′,N′,N″-pentamethyldiethyltriamine (PMDETA) (99%+), Cu(I)Cl (99.99%+), hydrazine hydrate, 3-(3,5,7,9,11,13,15-heptaiosbutylpentacyclo[9.5.1(3,9).1(5,15).1(7,13)]octasiloxan-1-yl)propyl methacrylate [MA POSS(isobutyl)], azoisobutylnitrile (AIBN) and ethyl 2-bromoisobutylrate (all from Aldrich) were used as received. Benzoyl chloride (from Fluka) was used as received. Methylene chloride (from VWR) was used as received. 2-Bromoisobutyrylbromide, triethylamine both were dried over CaH_2 before distillation and were stored and used under N_2 atmosphere after purification. THF and Toluene were distilled over sodium/benzophenone mixture.

2.1.2. Equipment

All NMR spectra were collected on a Bruker 300 MHz instrument and obtained from either $CDCl_3$ or CD_2Cl_2 solutions. ^{1}H NMR spectra (reported in ppm using the δ scale) were referenced to either residual $CHCl_3$ at 7.26 ppm or residual $CHDCl_2$ at 5.3 ppm. Gel Permeation Chromatography was performed with THF as mobile phase with a flow rate of 1 mL/min using Polymer Laboratories PL Gel 5 μm Mixed-D columns, Knauer K-501 HPLC Pump equipped with Knauer K-2301 differential refractometer detector and Knauer K-2600 dual wavelength UV Detector. Molecular weights were calibrated versus PMMA or PS standards. All FTIR spectra were obtained on a Perkin Elmer Spectrum One.

2.1.3. ATRP synthesis of PMA-POSS oligomers [39]

To a heat-dried 10 mL Schlenk flask with a magnetic stir bar were added Cu(I)Cl (10.5 mg, 0.106 mmol), THF (0.5 mL), and PMDETA (22.2 μL, 0.106 mmol). After the mixture was stirred for 10 min, MAPOSS (isobutyl) (1.00 g, 1.06 mmol), ethyl 2-bromoisobutyrate (15.55 μL, 0.106 mmol) and THF (1.0 mL) were added to the dark green solution of the catalyst and stabilizing agent. Three freeze-pump-thaw cycles were then performed to remove oxygen. After polymerization at 50 °C for 16 h, the reaction was cooled to room temperature and diluted with THF and passed through a wet activated neutral alumina column to remove the catalyst and stabilizing agent. The colorless and transparent dilute solution was concentrated by evaporation and precipitated in methanol and dried under vacuum overnight. Monomer residues were removed by Soxhlet extraction in methanol or acetonitrile for 5 days. The white polymer powder was vacuum dried.

^{1}H NMR ($CDCl_3$, 300 MHz): δ 0.54 ppm (d, 14H, SiCH_2CH$(CH_3)_2$), 0.58 ppm (t, 2H Si$CH_2CH_2CH_2$OC(O)–), 1.01 ppm (d, 42H, SiCH$_2$CH$(CH_3)_2$), 1.29 ppm (s, 6H, –$(CH_3)_2$C), 1.34 ppm (s, 3H, –$CH_2C(CH_3)$), 1.6 ppm (m, 2H Si$CH_2CH_2CH_2$OC(O)–), 1.8 ppm (m 7H, Si$CH_2CH(CH_3)_2$), 1.81 ppm (t, 3H CH_3CH_2OC(O)–), 1.91 ppm (s, 2H, –$CH_2C(CH_3)$), 3.9 ppm (t, 2H Si$CH_2CH_2CH_2$OC(O)–), 4.27 ppm (q, 2H, –CH_2OC(O)–). Gel permeation chromatography using THF as mobile phase gave M_n of 8480 g/mol (degree of polymerization (m) = 9) and PDI of 1.05.

Ethyl isobutyrate (phenyl) POSS PMA oligomers was synthesized by identical reaction and fully characterized. The GPC data is summarized in Table 1.

2.1.4. Synthesis of phthalimide POSS PMA samples and derivatives

ATRP was carried out using N-2-(2-(2-bromoisobutyryloxy) ethoxy)ethyl phthalimide (81.2 mg, 0.211 mmol) (synthesized as described by Lecolley et al.) [40] as initiator in similar conditions as described above. Yield: 1.65 g White powder (85%,

Table 1
M_n and PDI values of PMA and styryl POSS oligomers.

R group (periphery)	Ethyl isobutyrate–POSS g/mol (PDI)	Phthalimide–POSS g/mol (PDI)	Primary amine–POSS g/mol (PDI)
Isobutyl PMA	8480 (1.05)	–	–
Phenyl PMA	8250 (1.05)	–	–
Isobutyl PMA	–	6500 (1.05)	6200 (1.10)
Isobutyl styryl	–	7300 (1.07)	5800 (1.05)
Cyclohexyl styryl	–	5800 (1.08)	5700 (1.08)
Cyclopentyl styryl	–	4500 (1.08)	3500 (1.07)

0.12 mmol). ^{1}H NMR ($CDCl_3$, 300 MHz): δ 0.54 ppm (d, 8H, SiC*H*$_2$CH(CH$_3$)$_2$), 0.58 ppm (t, 2H SiC*H*$_2$CH$_2$CH$_2$OC(O)–), 1.01 ppm (d, 42H, SiCH$_2$CH(C*H*$_3$)$_2$), 1.29 ppm (s, 6H, –(CH$_3$)$_2$C), 1.34 ppm (s, 3H, –CH$_2$C(C*H*$_3$)), 1.6 ppm (m, 2H SiCH$_2$C*H*$_2$CH$_2$OC(O)–), 1.8 ppm (m 7H, SiCH$_2$C*H*(CH$_3$)$_2$), 1.91 ppm (s, 2H, –C*H*$_2$C(CH$_3$)), 3.72 ppm (t, 2H C*H*$_2$CH$_2$OC(O)–), 3.76 ppm (t, 2H, –OC*H*$_2$CH$_2$N–), 3.90 ppm (t, 2H, –NCH$_2$–), 3.9 ppm (t, 2H SiCH$_2$CH$_2$C*H*$_2$OC(O)–), 4.27 ppm (t, 2H, –CH$_2$OC(O)–), 7.70–7.86 ppm (m, 4H aromatic protons). Gel permeation chromatography (see Fig. 2) using THF as mobile phase gave M_n of 6500 g/mol (m = 7) and PDI of 1.05. IR 2953, 1729 (ester C=O stretch), 1464, 1383, 1366, 1332, 1228, 1087 (Si–O stretch), 836, 739 cm^{-1} (Scheme 1).

2.1.4.1. Conversion of phthalimide (i-butyl) POSS PMA to primary amine. Phthalimide (i-butyl) POSS PMA oligomer (0.5 g, 76.9 μmol) was dissolved in THF (10 mL) to which was added hydrazine hydrate (5 mL, 100 mmol). The solution was refluxed for 40 h. Deprotection was accompanied by the formation of white precipitate of phthalhydrazide. The salt was separated by filtration; polymer was then precipitated in methanol. The removal of solvent in vacuo gave the desired product, which was further dried under high vacuum. Yield: 0.281 g (57%, 44.1 μmol) white powder. ^{1}H NMR ($CDCl_3$, 300 MHz): δ 0.54 ppm (d, 14H, SiC*H*$_2$CH(CH$_3$)$_2$), 0.58 ppm (t, 2H SiC*H*$_2$CH$_2$CH$_2$OC(O)–), 1.01 ppm (d, 42H, SiCH$_2$CH(C*H*$_3$)$_2$), 1.29 ppm (s, 6H, –(CH$_3$)$_2$C), 1.34 ppm (s, 3H, –CH$_2$C(C*H*$_3$)), 1.6 ppm (m, 2H SiCH$_2$C*H*$_2$CH$_2$OC(O)–), 1.8 ppm (m 7H, SiCH$_2$C*H*(CH$_3$)$_2$), 1.91 ppm (s, 2H, –C*H*$_2$C(CH$_3$)), 2.8 ppm (t, 2H, NH$_2$), 3.72 ppm (t, 2H C*H*$_2$CH$_2$OC(O)–), 3.76 ppm (t, 2H, –OC*H*$_2$CH$_2$N–), 3.90 ppm (t, 2H, –NCH$_2$–), 3.9 ppm (t, 2H

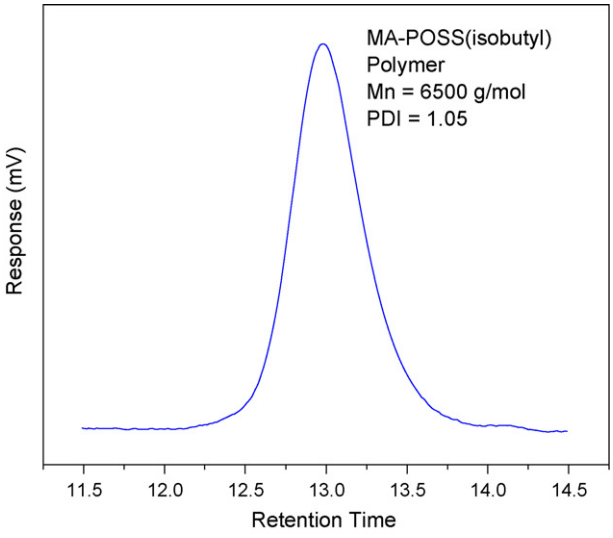

Fig. 2. GPC of MA-POSS(isobutyl) polymer.

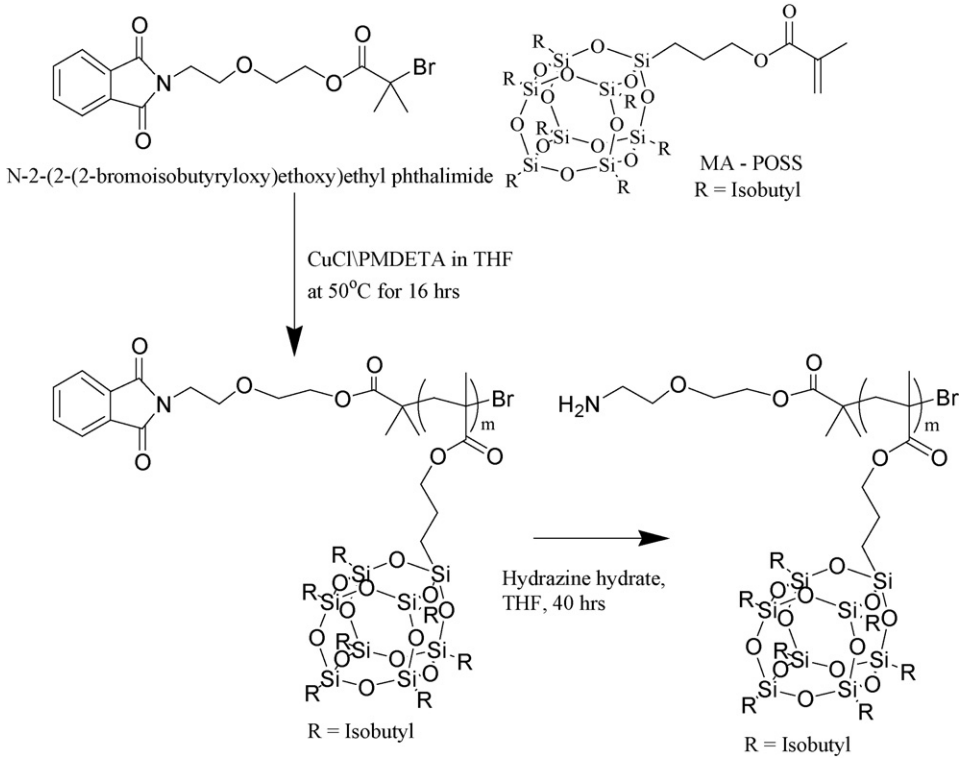

Scheme 1. Synthesis of Isobutyl POSS PMA polymers using phthalimide initiator by ATRP.

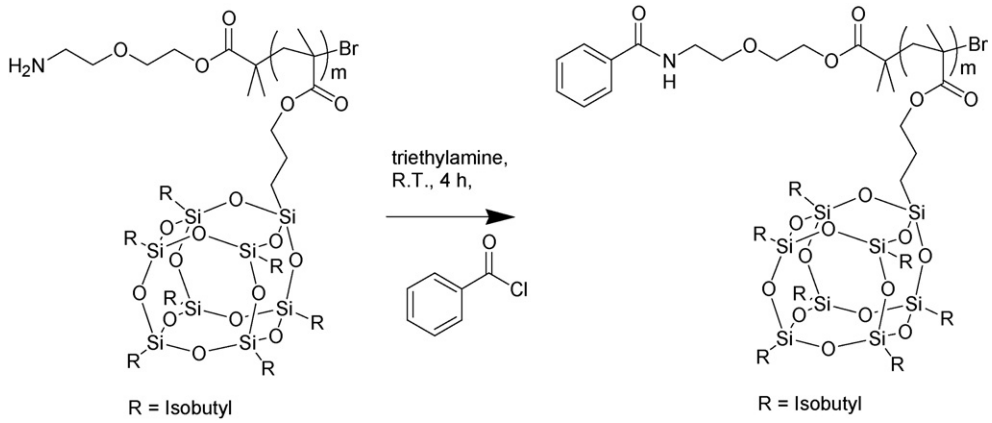

Scheme 2. Synthesis of benzoyl isobutyl POSS PMA oligomer.

$SiCH_2CH_2CH_2OC(O)$–), 4.27 ppm (t, 2H, $–CH_2OC(O)$–). Gel permeation chromatography using THF as mobile phase gave M_n of 6200 g/mol (m = 7) and PDI of 1.1, IR 2953 (N–H stretch), 1729 (ester C=O stretch), 1459,1366,1266,1087 (Si–O stretch), 834, 735 cm^{-1}.

Conversion from phthalimide to primary amine was studied by GPC with UV detector, ^1H NMR and IR spectroscopy (see Supplementary Material). UV-active phthalimide compounds were observed in GPC trace using the UV detector at 254 nm. After the deprotection, the disappearance of GPC trace at 254 nm confirmed the removal of the protecting group. In ^1H NMR too there was no signal detected between δ 7.00 and 8.00 ppm further confirming the deprotection of the protecting group. In ^1H NMR and the IR spectrum the primary amine peaks were observed at δ 2.8 ppm and 3000–3300 cm^{-1} respectively.

2.1.4.2. Reaction of primary amine with benzoyl chloride. H_2N (i-butyl) POSS PMA oligomer (50 mg, 7.6 μmol) was dissolved in methylene chloride and triethylamine was used as base. Benzoyl chloride (18 μL, 153 μmol) (Ratio polymer: benzoyl chloride 1:20) was added and reaction was continued for 6 h. The solution was washed with water (3× 10 mL) and the solvent was removed in vacuo. The white powder was washed with methanol to remove the benzoic acid formed and then vacuum dried. Yield = 38 mg (76%, 5.7 μmol). ^1H NMR (CD_2Cl_2, 300 MHz): δ 0.54 ppm (d, 14H, $SiCH_2CH(CH_3)_2$), 0.58 ppm (t, 2H $SiCH_2CH_2CH_2OC(O)$–), 1.01 ppm (d, 42H, $SiCH_2CH(CH_3)_2$), 1.29 ppm (s, 6H, $–(CH_3)_2C$), 1.34 ppm (s, 3H, $–CH_2C(CH_3)$), 1.6 ppm (m, 2H $SiCH_2CH_2CH_2OC(O)$–), 1.8 ppm (m 7H, $SiCH_2CH(CH_3)_2$), 1.91 ppm (s, 2H, $–CH_2C(CH_3)$), 3.72 ppm (t, 2H $CH_2CH_2OC(O)$–), 3.76 ppm (t, 2H, $–OCH_2CH_2N$–), 3.90 ppm (t, 2H, $–NCH_2$–), 3.9 ppm (t, 2H $SiCH_2CH_2CH_2OC(O)$–), 4.27 ppm (t, 2H, $–CH_2OC(O)$–), 7.4 ppm (t, 1H, NHCO), 7.70–7.8 ppm (m, 4H aromatic protons). Gel permeation chromatography using THF as mobile phase gave an M_n of 6800 g/mol (m = 7) and PDI of 1.06. IR 2953, 2870, 1785 (amide C=O stretch), 1726 (ester C=O stretch), 1599 (amide –NHCO stretch) 1464, 1451, 1401, 1383, 1366, 1322, 1228, 1211, 1170, 1087 (Si–O stretch), 996, 836, 739, 702 cm^{-1} (Scheme 2).

In ^1H NMR, peaks at δ 7.7–7.8 ppm showed the presence of the benzoyl group. The newly formed amide linkage was observed both in the ^1H NMR and IR spectra at δ 7.4 ppm and 1599 cm^{-1} respectively. The detection of the amide bond formed by the reaction of benzoyl chloride with primary amine confirmed the presence of amine group in PMA POSS oligomers.

2.1.5. Synthesis of POSS PMA samples using free radical polymerization

To compare with ATRP synthesized oligomers, POSS oligomers were also synthesized by conventional free radical polymerization using about 10 mol% AIBN to promote the formation of oligomers. To an oven dried round bottom flask was added (i-butyl) PMA POSS (0.210 g, 0.22 mmol), AIBN (3.1 mg, 0.018 mmol) and degassed toluene (1.7 mL). The reaction was carried out for 2 days at 60 °C. The oligomeric mixture was then precipitated in methanol and dried under vacuum overnight to yield a white powder. (Cp) POSS PMA oligomers were synthesized by an identical reaction and characterized by mass spectrometry.

2.1.6. ATRP synthesis of phthalimide Styryl-POSS oligomers

Synthesis of Styryl-POSS oligomers were carried out in a procedure similar to the one described above for phthalimide POSS PMA oligomers (see Supplementary Material).

2.2. Mass spectrometry

Matrix-assisted laser desorption/ionization (MALDI) spectra were recorded on either a Bruker Reflex-III MALDI time-of-flight (TOF) instrument or on a Bruker Ultraflex III MALDI-TOF-TOF tandem mass spectrometer (Bruker Daltonics, Billerica, MA). These instruments are equipped with a N_2 and Nd:YAG laser, respectively. The synthesis and other applications of the 4,4′-dihydroxyoctofluoroazobenzene (traditionally denoted as **M4**) was discussed in detail in Ref. [38]. The matrix was dissolved in tetrahydrofuran (THF) (ca. 10 mg/mL) and this matrix solution was mixed with the THF solutions (ca. 1 mg/mL) of the POSS polymer analytes in a 10:1 ratio. Both the linear (lower resolution but larger mass range) and the reflectron (higher resolution but smaller mass range) ion detection modes were applied. The laser power was varied to obtain the best quality spectra but avoid significant fragmentation in the MS studies. MS/MS tandem experiments were performed on the Ultraflex III MALDI TOF-TOF instrument by using the LIFT [41] technique and applying higher laser powers than for the MS studies. No significant changes in the fragmentation efficiency were observed with or without pulsing the nitrogen collision gas in the selected ion path.

Electrospray (nanospray) ionization (ESI)-MS. Polymer samples were electrosprayed using a homebuilt nanoESI source from a solution of 50:50 MeOH:H_2O and analyzed on quadrupole time-of-flight mass spectrometer (modified Waters Q-TOF 2 that has been described elsewhere [42]). The electrospray voltage was set at 1.5 kV and the cone voltage was varied between 35 and 100 V. Pressure in the source region of the instrument was regulated with a speedivalve on the roughing pump and optimized for highest ion transmission over the entire mass range, typically between 1×10^{-3} mbar and 1×10^{-2} mbar in the source hexapole chamber. The TOF pressure was 1×10^{-2} mbar. For MS/MS measurements Ar was used as a collision gas and the laboratory collision energy

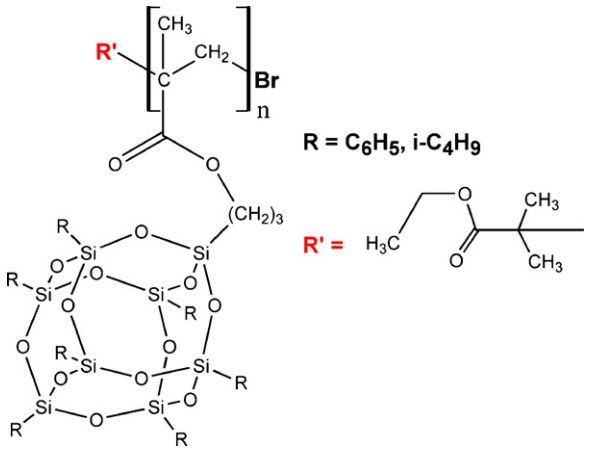

Fig. 3. Ethyl isobutyrate POSS PMA oligomers synthesized using ATRP techniques.

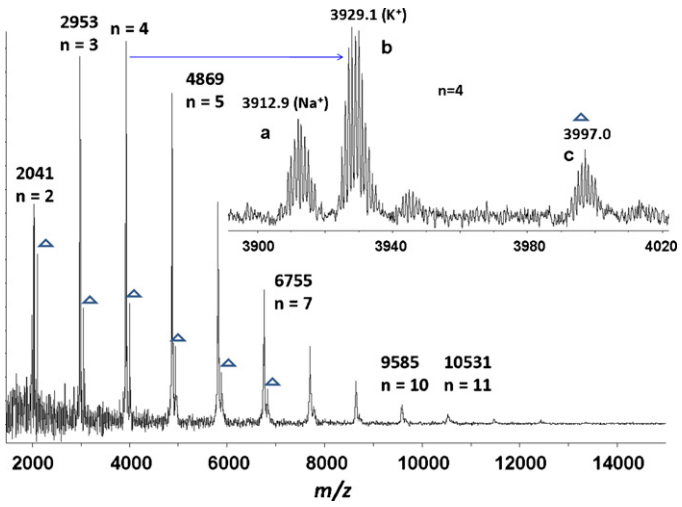

Fig. 5. Ethyl isobutyrate Isobutyl POSS PMA MALDI mass spectrum using 4,4′-dihydroxyoctofluoroazobenzene matrix. Typical series (**a–c**) shown in expansion in region of m/z = 3900–4040.

was determined by the potential difference between the (selection) quadrupole and the collision cell. All spectra were processed with minimal smoothing using MassLynx software (Waters).

3. Results and discussion

3.1. POSS PMA oligomers

The simplest series of POSS PMA oligomers include the isobutyl and phenyl oligomers, synthesized by the ATRP method as well as the free radical synthesized materials. These will be discussed in turn.

3.1.1. CH_3CH_2OOC-$C(CH_3)_2$-[(i-butyl)$_7T_8$propylmethacrylate]$_n$-Br

The generalized structure of this ethyl isobutyrate POSS PMA oligomer is given in Fig. 3. It is the product of an ATRP synthesis and the parent is terminated with a chain-propagating bromine atom. NMR and GPC analysis, coupled with mass spectrometry are consistent with this structure. Focusing on the MALDI and ESI results (see ESI and MALDI spectra in Figs. 4 and 5, respectively) different ion series in the mass spectra are clearly evident and give evidence for the range of oligomers synthesized in the ATRP method In fact, this series represents the molecular mass limit under the ATRP conditions employed. The repeat mass of 944 is common in both the ESI and MALDI spectra and corresponds to the structure shown. In the ESI spectrum (Fig. 4) the two closely spaced most intense peaks can be assigned to sodiated and potassiated parent species, formed by adventitious ions present. The terminal Br is replaced by an –OH group. MSMS of the 2042 peak shows fragmentation corresponding to two paths (spectrum not shown). The first path involves loss of (i-butyl)$_7T_8(CH_2)_3OCO$ and the second to loss of (i-butyl)$_7T_8(CH_2)_3O$ fragments. This provided guidance in the interpretation of the MALDI spectrum.

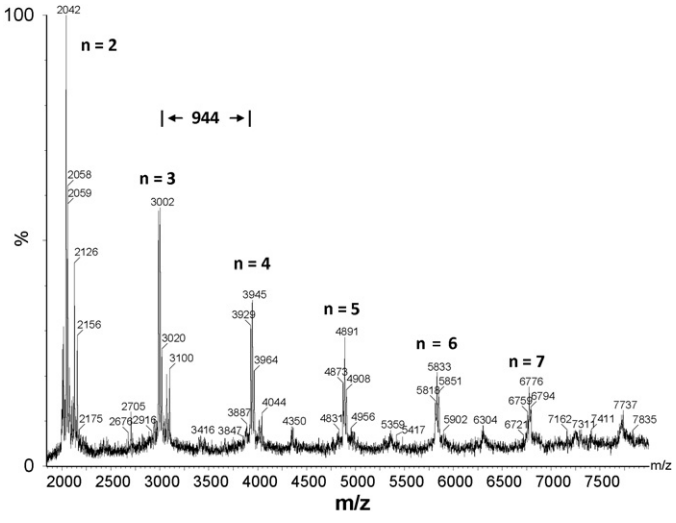

Fig. 4. ESI mass spectrum of CH_3CH_2OOC-$C(CH_3)$-[(i-butyl)$_7T_8$propylmethacrylate]$_n$. Most intense peaks are assigned to sodiated and potassiated parent species, the terminal Br being replaced with OH.

Fig. 5 gives the MALDI spectrum obtained in the linear mode and shows a progression of peaks out to n = 12 with the terminal Br replaced by an H atom. The inset is an expansion of the typical set of three peaks centered around m/z ~3929 with clearly defined isotope splitting. The peak **a** at m/z = 3913 is the sodiated species while the peak **b** at 3929 is the potassiated species. The less intense third peak **c** (e.g., m/z 3997) of the repeating series can be assigned to the sodiated n + 1 oligomer minus an (i-bu)$_7T_8(CH_2)_3$– fragment which is replaced by a hydrogen. The fragmentation occurs due to the thermal elimination reaction in esters at high temperature in the gaseous state. This assignment has been confirmed by MSMS spectra of the m/z 3929 and the analogous 2982 peaks which show fragmentations corresponding to the loss of one or more (i-bu)$_7T_8(CH_2)_3$– units from the PMA backbone (spectrum not shown). The theoretical isotope distribution pattern for these two peaks fits the experimental distribution very closely, further supporting our assignment.

3.1.2. CH_3CH_2OOC-$C(CH_3)_2$-[(Phenyl)$_7T_8$ propylmethacrylate]$_n$-Br

This closely related material was well characterized by NMR, GPC and mass spectrometry. The MALDI mass spectrum when R = phenyl is shown in Fig. 6 [43]. The repeat unit is 1083 amu. Clearly resolved series are again observed out to n = 12, even though the synthesis stoichiometry was targeted for an octamer. GPC data (see Table 1) shows that the average molecular weight of ~8250 does correspond to this stoichiometry and this is roughly reflected in the MALDI mass distribution which is maximum in the hexamer region. Similar to the isobutyl POSS PMA species above, the two most intense peaks (series **a** and **b**) in an n-mer set such as depicted in the inset can be assigned to adventitious sodiated and potassiated parent species that have Br replaced by an H-atom. The intense third peak of the repeating series (e.g., m/z ~7808,

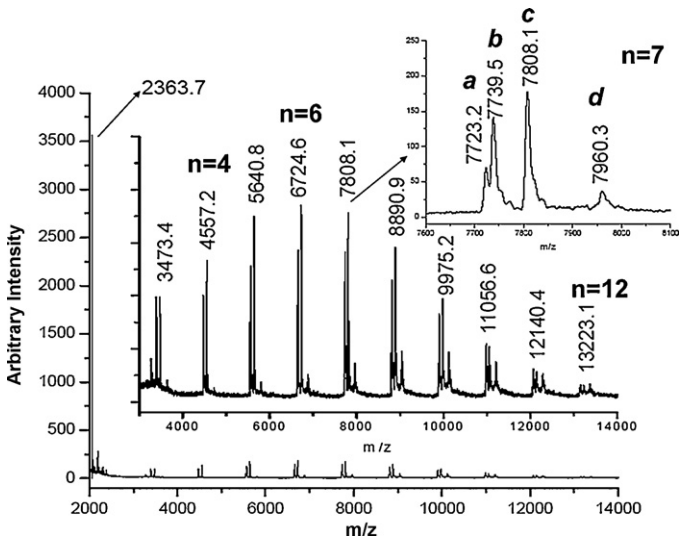

Fig. 6. Phenyl POSS PMA MALDI mass spectrum using 4,4′-dihydroxyoctoflyoroazobenzene matrix. Typical series (**a**–**d**) shown in expansion in region of $m/z = 7800$.

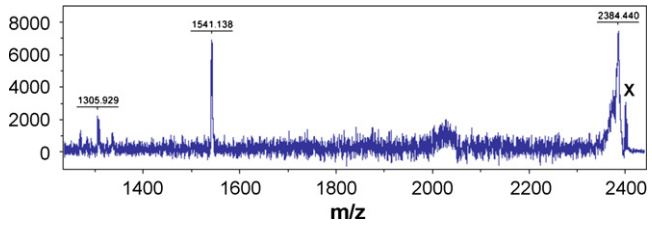

Fig. 8. MSMS MALDI spectrum of phthalimido-Isobutyl POSS PMA using 4,4′-dihydroxyoctofluoroazobenzene matrix for the m/e 2397 peak (**x**).

series **c**) can be assigned to the sodiated $(n+1)$ oligomer minus a $(\text{phenyl})_7T_8(CH_2)_3-$ fragment with the terminal Br replaced by an H-atom. Relative intensity of this peak compared with the parent ion increases with chain length since the increasing number of POSS side chains increases the probability of their loss by fragmentation. The fourth peak of each sub-series (e.g., m/z ~7960, series **d**) grows in relative intensity and is best interpreted as the loss of a second $(\text{phenyl})_7T_8(CH_2)_3-$ fragment from the $(n+2)$ oligomer.

The ESI mass spectrum is shown in Fig. 7. A somewhat different series of ions arises arise under electrospray conditions in contrast to the isobutyl case. The major mass peaks at m/z 3440, 4524 and 5607 can be accounted for by protonation of the parent bromo species rather than replacement of the terminal Br by –OH. The best explanation of the peaks at m/z 3163 and 4246 is the above potassiated species accompanied by fragmentation involving loss of a PhSiO–OSiPh (edge) from *one* of the 3-mer or 4-mer T_8 cages.

3.1.3. $C_6H_4(CO)_2NCH_2CH_2OCH_2CH_2OOC\text{-}C(CH_3)_2\text{-}(i\text{-}Butyl)_7T_8propylmethacrylate]_n–Br$

In an attempt to obtain NH_2-substituted series of oligomers, intermediate phthalimido-POSS PMA materials were synthesized which gave quite good MALDI-TOF mass spectra.

The MALDI-TOF mass spectrum of this phthalimidoester oligomer is quite similar to the ethyl isobutyrate (i-butyl)POSS and phenyl POSS PMA species already discussed. The total spectrum is characterized by the isobutyl POSS repeat unit of 944 amu and clearly resolved series of three peaks observed out to $n = 10$, for the nominal octamer.

The mass spectra of the phthalimidoesters does show some unique features due to fragmentation of the parent ion.

Assignment of fragment peaks is illustrated in Fig. 8 which displays the MALDI-TOF-TOF MSMS spectrum of one the highest mass trimer fragments at m/z 2397. The m/z 1541 peak corresponds to the loss of a $(\text{ibu})_7T_8(CH_2)_3-$ fragment from one of the side chains. The broad hump at ~2020 corresponds to some metastable fragmentation the origin of which is not well understood. The ion at m/z 2397 itself by similar analysis is the disodiated parent ion minus a $(\text{ibu})_7T_8(CH_2)_3-$ cage fragment, the terminal Br being replaced by a hydrogen.

3.1.4. $NH_2CH_2CH_2OCH_2CH_2OOCC(CH_3)_2\text{-}[(i\text{-}Butyl)_7T_8propylmethacrylate]_n\text{-}Br$

This series of oligomers is prepared by converting this phthalimide material to the amine as described in the experimental section. The interpretation of the MALDI spectrum is complicated due to ion chemistry in which the terminal amine reacts with the ester linkages of the oligomer backbone, perhaps producing a series of

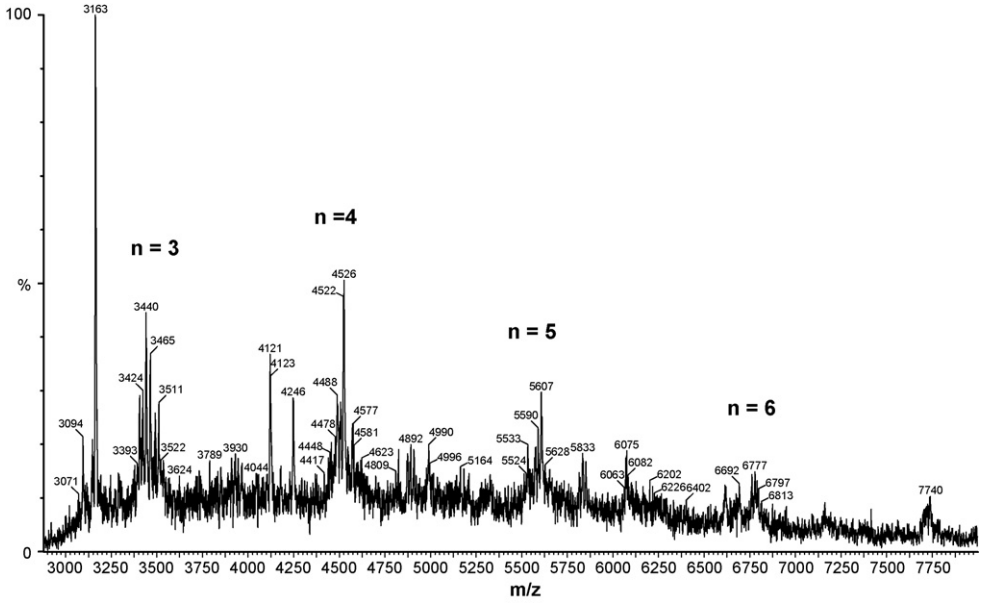

Fig. 7. ESI mass spectrum of $CH_3CH_2OOC\text{-}C(CH_3)\text{-}[(\text{phenyl})_7T_8\text{propylmethacrylate}]_n\text{-}Br$. The largest peak in each series up to $n = 6$ corresponds to protonation of the parent.

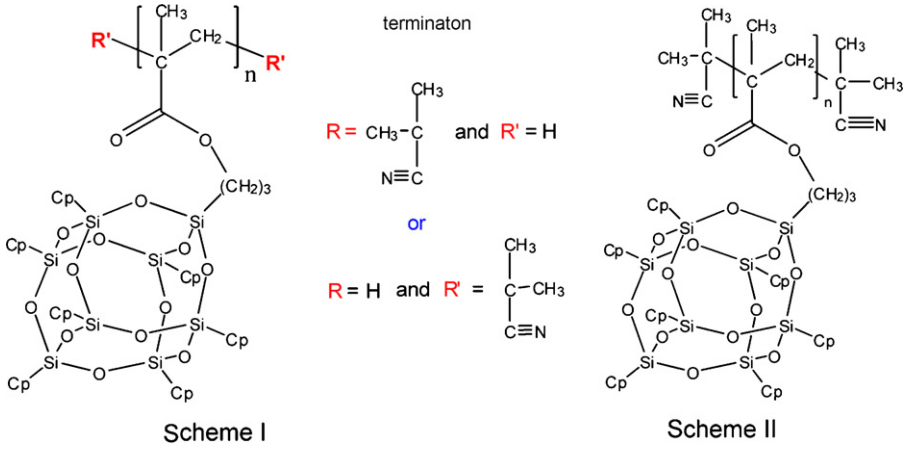

Scheme 3. Free radical termination in cyclopentyl POSS PMA oligomers. Scheme I: single i-butylnitrile; Scheme II: two i-butylnitrile groups. Cp = cyclopentyl.

cyclic amides in the process. Complex spectra result in which the dominant peaks seem to arise by loss of cage fragments such as C_4H_9Si, C_4H_9SiO, and $C_4H_9SiO_2$.

A weak series of high *m*/*z* peaks can be observed, however, which represent the oligomer series. A potassiated parent ion can be confidently assigned with the terminal bromine replaced with a hydrogen. Sodiated peaks are occasionally observed. The spectra and assignments are tabulated in the Supplementary Material, section D.

3.1.5. $[(R)_7T_8$Propylmethacrylate$]_n[(CH_3)_2CCN]_{m=1,2}$; R = i-butyl and cyclopentyl (Cp)

Isobutylnitrile isobutyl and cyclopentyl (Cp) POSS PMA materials were synthesized using a free radical procedure employing various mole ratios of azoisobutylnitrile. Scheme 3 shows the variety of ways which these oligomers (Cp in this example) can be terminated, either by an H atom or the isobutylnitrile radical. The mass spectra obtained for the range of syntheses were of very good quality and give evidence for oligomers out to the pentamer with peaks clearly assigned to one or two isobutylnitrile terminal groups. Both sodiated and potassiated species are observed with no di-H termination evident except for the dimer. This is expected for relatively large amounts of AIBN used in the synthesis. The mass spectrum repeat unit is 1028 for the cyclopentyl materials and 944 for the isobutyl species, based on the monomer.

The isobutyl oligomer also shows a series of very low intensity peaks evident for masses corresponding to the presence of *three* isobutyl nitrile groups. This occurs when higher concentration of the initiator is present and is due to abstraction of a hydrogen radical from the backbone or periphery (R) group and subsequent reaction with a third AIBN radical. While this could happen at any of the backbone hydrogen positions, substitution is more likely at the unique tertiary vinyl carbon which already has one isobutylnitrile moiety bonded. Spectra and assignments are tabulated in the Supplementary Material, sections E-G.

3.2. POSS styryl oligomers

Styryl oligomers also synthesized by ATRP provided an important contrast to the PMA POSS oligomers already described.

3.2.1. $C_6H_4(CO)_2NCH_2CH_2OCH_2CH_2OOC$-$C(CH_3)_2$-$R)_7T_8(C_6H_4CHCH_2)]_n$–Br; R = i-Butyl, cyclopentyl (Cp), and cyclohexyl (Cy)

The phthalimidoester styrylPOSS intermediates gave very good to excellent MALDI-TOF mass spectra, once again giving evidence for ion chemistry products rather than simple parent ions. These species are characterized by oligomer repeat units of 919, 1003 and 1001 mass units for the i-butyl, cyclopentyl and cyclohexyl R-groups, respectively. Fig. 9 shows a comparison between spectra obtained in the new matrix and the standard 2-(4hydroxyphenylazo)benzoic acid (HABA). The signal-to-noise ratio and resolution show a significant improvement compared to the standard matrix. In fact, this is one of the few examples of POSS oligomers for which any MALDI spectrum could be obtained with a standard matrix.

The spectra of the styryl species are similar to the PMA materials, but are more complex and show some very interesting differences. These differences are primarily due to two steric factors, namely the nature of the all carbon backbone of the styryl POSS series versus the ester backbone of the POSS PMAs, and the effect of the R-group size on the conformation of the backbone and ability to protect the terminus.

The styryl POSS oligomer spectrum (Fig. 9) is typified by the cyclopentyl phthalimidoester (see Supplementary Material, section H-J). Potassiated parent ions ($M+K^+$) are observed, but are of low intensity. Assigned peaks show multiplets corresponding to sodiated and potassiated species (e.g., 2354, 3369, and 4357) which have lost the terminal Br atom and added an H atom as in the PMA series. The most intense peaks cannot be assigned to simple molecular ion derived species, but correspond to the products of ion chemistry in the source. For example, when a terminal Br atom is lost, it is possible for the radicals produced to couple and we observe mass peaks consistent with head-to-head coupling of these fragments to generate protonated, sodiated and potassiated dimers (peaks at 2637, 3660, 4646, 4660, 5642 and 6647) up to 6-mers. The cyclopentyl group seems to be of optimum size to "straighten" out the backbone so that the terminus of separate fragments are exposed and can bond. Since the presence of a cation will not influence the conformation of the styryl backbone as happens in the case of the PMAs via coordination to carbonyl groups, backbone extension would be facilitated. For the larger R = cyclohexyl, only dimer and trimer coupling products are observed and none of the higher oligomers present in the Cp mass spectrum. This is presumably due to steric reasons. When R = Cy and $n > 3$, more crowded species result which "protect" the terminus so that it cannot couple. Instead, it adds a small H atom. Assignments involving analyte/matrix complexes can be ruled out for all R-groups since all mass peaks are common to spectra obtained in both 4,4′-dihydroxyoctafluoroazobenzene and HABA matrices.

In the case of R = i-butyl, only dimer and trimer coupling reaction products are evident, similar to the R-cyclohexyl oligomers, but for different reasons. The i-butyl group is much small than

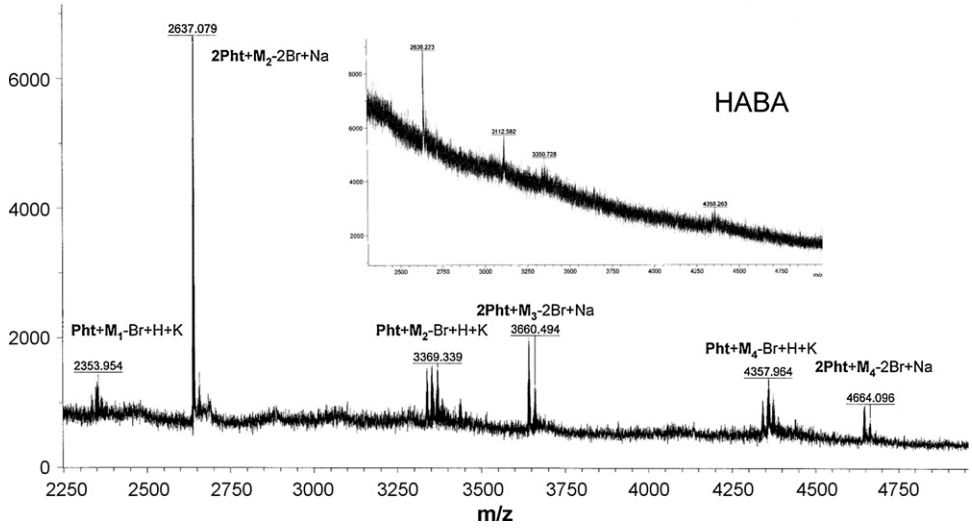

Fig. 9. MALDI mass spectra of (Cp) styryl POSS in 4,4′-dihydroxyoctofluoroazobenzene. Inset shows spectrum in HABA matrix.

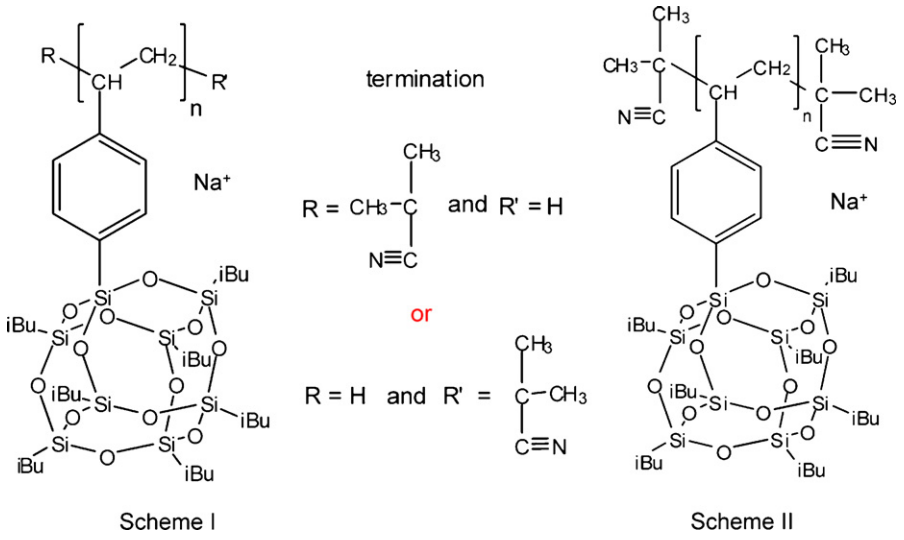

Scheme 4. Free radical termination in i-butyl POSS styryl oligomers. Scheme I: single i-butylnitrile; Scheme II: two i-butylnitrile groups.

the cyclopentyl or cyclohexyl groups. We have previously observed that cages have a tendency to cluster due to van der Waals interactions which become more important as the oligomer get larger [14]. A small R-group enables closer association of the cages as shown by our modeling, the effect of which is to cause the backbone to wrap around rather than to "straighten" and the species to become very compact. The over-all effect is the same as a large R = cyclohexyl group blocking the terminus; if the terminus is buried in the center of compacted oligomer it cannot couple with another radical. It will be less accessible, especially for longer chains. High resolution ion mobility studies will allow us to further characterizes such structures.

3.2.2. $[(i\text{-}Butyl)_7T_8(C_6H_4CHCH_2)]_n[(CH_3)_2CCN]_{m=1,2,3}$

Isobutylnitrile styryl-POSS oligomers were synthesized in the same way as the POSS-propylmethacrylates under free radical conditions with the initiator concentration ranging from 2 to 30 mol%. Scheme 4 depicts the synthetic routes which give rise to two isobutylnitrile terminated species corresponding to the most intense observed peak (B) in the mass spectrum (see Fig. 10). The same series of very low intensity peaks corresponding to the presence of *three* isobutylnitrile groups similar

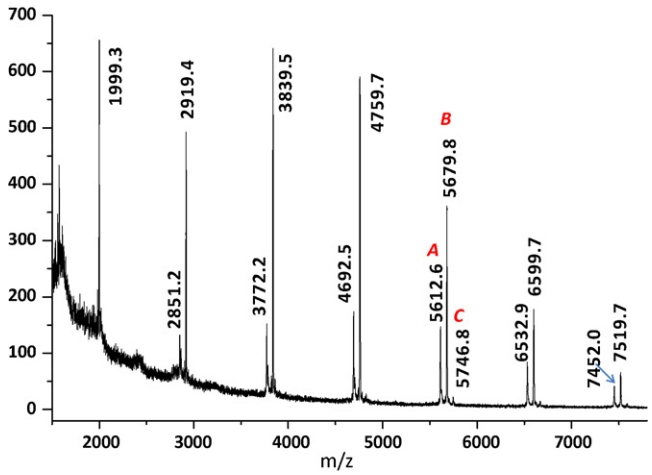

Fig. 10. Isobutylnitrile (i-butyl)styrylPOSS MALDI mass spectrum using 4,4′-dihydroxyoctofluoroazobenzene matrix. Labels **A, B,** And **C** correspond to 1–3 isobutylnitrile groups.

to that seen previously in the isobutylPOSS PMA spectra is evident.

4. Conclusions

We have succeeded in obtaining ESI and MALDI mass spectra on a variety of PMA and styryl POSS oligomers, in some cases out to mass ~16,000. MALDI spectra were greatly enhanced with the use of a new matrix, 4,4′-dihydroxyoctafluoroazobenzene. ATRP syntheses were much more effective than free radical procedures in creating oligomers up to ~13 repeat units. ESI and MALDI mass spectra of the ATRP products rarely gave true molecular ion peaks for any oligomer; rather the terminal halogen was invariably replaced with a hydroxyl or hydrogen atom, respectively. Single atom substitutions are not expected to change the conformation relative to the parent species.

For the PMA series, the most intense peaks observed in the mass spectra correspond to simple sodiated or potassiated species related to the substituted parent ion. Less intense peaks arise from fragmentations (generally loss of one or more of the POSS side chains) and recombinations, since these processes have relatively low probabilities. These are not of primary structural interest since they represent degraded parent oligomers, but may give insight into how side chains affect backbone conformation. MSMS was used to assign the major peaks for several sets of oligomers, and by analogy, to develop a consistent explanation of the observed spectra for the PMA oligomers studied.

The all-carbon backbone of the styryl materials was resistant to fragmentation but the mass spectra obtained did show recombinations arising from the loss of the terminal Br atom not observed with the POSS PMAs. Coupling of radicals produced by Br atom loss gave rise to multimers. Differences in these ion chemistry products allowed us to draw conclusions about the structures of the styryl species.

Free radical methods did not give materials with more than seven repeat units in any case studied. Termination occurs via a H atom and/or one or two isobutylnitrile moieties from the initiator depending on the amount present in the synthesis.

The intensity of peaks in the MALDI-TOF-TOF spectra in most cases is sufficient to obtain ion mobility data. We will report structural investigation in a subsequent paper.

Supplementary material available

Information which includes characterization of the styryl oligomers and detailed assignments of the mass spectra reported in this paper is available free of charge via the Internet at http://pubs.acs.org.

Acknowledgments

The Air Force Office of Scientific Research under grant F49620-03-1-0046 (M.T.B.) and NSF under grant DMR-0239475 (E.B.C.) are gratefully acknowledged for support of this work. We also thank the NAS/NRC Senior Associateship Program for fellowship support of S.E.A. Finally we thank Christopher M. Jones of the Wysocki group at the University of Arizona for obtaining the ESI spectra reported.

Appendix A. Supplementary data

Supplementary data associated with this article can be found, in the online version, at doi:10.1016/j.ijms.2010.02.013.

References

[1] M.G. Voronkov, V.I. Lavrentyev, Polyhedral oligosilsesquioxanes and their homo derivatives, Top. Curr. Chem. 102 (1982) 199–236.
[2] P.A. Agaskar, New synthetic route to the hydridospherosiloxanes O_h-$H_8Si_8O_{12}$ and D_{5h}-$H_{10}Si_{10}O_{15}$, Inorg. Chem. 30 (1991) 2707–2708.
[3] P.A. Agaskar, W.G. Klemperer, The higher hydridospherosiloxanes - synthesis and structures of $H_nSi_nO_{1.5n}$ (N = 12, 14, 16, 18), Inorg. Chim. Acta 229 (1995) 355–364.
[4] R.H. Baney, M. Itoh, A. Sakakibara, T. Suzuki, Silsesquioxanes, Chem. Rev. 95 (1995) 1409–1430.
[5] J.D. Lichtenhan, Polyhedral oligomeric silsesquioxanes—building-blocks for silsesquioxane-based polymers and hybrid materials, Comments Inorg. Chem. 17 (1995) 115–130.
[6] J.D. Lichtenhan, in: J.C. Salamore (Ed.), Polymeric Materials Encyclopedia, CRC Press, NY, 1996, pp. 7769–7778.
[7] G.Z. Li, L.C. Wang, H.L. Ni, C.U. Pittman, Polyhedral oligomeric silsesquioxane (POSS) polymers and copolymers: a review, J. Inorg. Organomet. Polym. 11 (2001) 123–154.
[8] G.Z. Li, C.U. Pitman, in: A.S. Abd El Aziz, C.E. Carraher, C.U. Pittman, M. Zeldin (Eds.), Macromolecules Containing Metals and Metal-like Elements, Vol. 4 Group IVA Polymers, John Wiley & Sons, Hoboken, NJ, 2005, pp. 79–131.
[9] S.H. Phillips, T.S. Haddad, S.J. Tomczak, Developments in nanoscience: polyhedral silsesquioxane (POSS)-polymers oligomeric, Curr. Opin. Solid State Mater. Sci. 8 (2004) 21–29.
[10] J. Wu, P.T. Mather, POSS polymers: physical properties and biomaterials applications, Polym. Rev. 49 (2009) 25–63.
[11] K. Pielichowski, J. Njuguna, B. Janowski, J. Pielichowski, Polyhedral oligomeric silsesquioxanes (POSS)-containing nanohybrid polymers, Adv. Polym. Sci. 201 (2006) 225–296.
[12] P.D. Lickiss, F. Rataboul, Fully condensed polyhedral oligosilsesquioxanes (POSS): from synthesis to application, Adv. Organomet. Chem. 57 (2008) 1–116.
[13] S.E. Anderson, C. Mitchell, T.S. Haddad, A. Vij, J.J. Schwab, M.T. Bowers, Structural characterization of POSS siloxane dimer and trimer, Chem. Mater. 18 (2006) 1490–1497.
[14] S.E. Anderson, E.S. Baker, C. Mitchell, T.S. Haddad, M.T. Bowers, Structure of hybrid polyhedral oligomeric silsesquioxane propyl methacrylate oligomers using ion mobility mass spectrometry and molecular mechanics, Chem. Mater. 17 (2005) 2537–2545.
[15] W.E. Wallace, C.M. Guttman, J.M. Antonucci, Molecular structure of silsesquioxanes determined by matrix-assisted laser desorption/ionization time-of-flight mass spectrometry, J. Am. Soc. Mass Spectrom. 10 (1999) 224–230.
[16] M. Farahani, J.M. Antonucci, C.M. Guttman, Analysis of the interactions of a trialkoxysilane with dental monomers by MALDI-TOF mass spectrometry, Polym. Prepr. (Am. Chem. Soc., Div. Polym. Chem.) 45 (2004) 350–351.
[17] M. Farahani, W.E. Wallace, J.M. Antonucci, C.M. Guttman, Analysis by mass spectrometry of the hydrolysis/condensation reaction of a trialkoxysilane in various dental monomer solutions, J. Appl. Polym. Sci. 99 (2006) 1842–1847.
[18] W.E. Wallace, C.M. Guttman, J.M. Antonucci, Polymeric silsesquioxanes: degree-of-intramolecular-condensation measured by mass spectrometry, Polymer 41 (1999) 2219–2226.
[19] R.J.J. Williams, R. Erra-Balsells, Y. Ishikawa, H. Nonami, A.N. Mauri, C.C. Riccardi, UV-MALDI-TOF and ESI-TOF mass spectrometry characterization of silsesquioxanes obtained by the hydrolytic condensation of (3-glycidoxypropyl)trimethoxysilane in an epoxidized solvent, Macromol. Chem. Phys. 202 (2001) 2425–2433.
[20] D.P. Fasce, R.J.J. Williams, R. Erra-Balsells, Y. Ishikawa, H. Nonami, One-step synthesis of polyhedral silsesquioxanes bearing bulky substituents: UV-MALDI-TOF and ESI-TOF mass spectrometry characterization of reaction products, Macromolecules 34 (2001) 3534–3539.
[21] M. Valencia, W. Dempwolf, F. Guenzler, O. Knoepfelmacher, G. Schmidt-Naake, Synthesis and characterization of silsesquioxane prepolymers bearing phenyl and methacryloxypropyl groups obtained by cohydrolysis, Macromolecules 40 (2007) 40–46.
[22] N. Auner, B. Ziemer, B. Herrschaft, W. Ziche, P. John, J. Weis, Structural studies of novel siloxysilsesquioxanes, Eur. J. Inorg. Chem. (1999) 1087–1094.
[23] P. Eisenberg, R. Erra-Balsells, Y. Ishikawa, J.C. Lucas, A.N. Mauri, H. Nonami, C.C. Riccardi, R.J.J. Williams, Cagelike precursors of high-molar-mass silsesquioxanes formed by the hydrolytic condensation of trialkoxysilanes, Macromolecules 33 (2000) 1940–1947.
[24] M. Karas, R. Krueger, Ion formation in MALDI: the cluster ionization mechanism, Chem. Rev. 103 (2003) 427–439.
[25] R. Knochenmuss, Ion formation mechanisms in UV-MALDI, Analyst 131 (2006) 966–986.
[26] E.S. Baker, J. Gidden, D.P. Fee, P.R. Kemper, S.E. Anderson, M.T. Bowers, 3-Dimensional structural characterization of cationized polyhedral oligomeric silsesquioxanes (POSS) with styryl and phenylethyl capping agents, Int. J. Mass Spectrom. 227 (2003) 205–216.
[27] P.R. Gidden, E. Kemper, D.P. Shammel, S. Fee, S.E. Anderson, M.T. Bowers, Application of ion mobility to the gas-phase conformational analysis of polyhedral oligomeric silsesquioxanes (POSS), Int. J. Mass Spectrom. 222 (2003) 63–73.
[28] E.S. Baker, J. Gidden, S.E. Anderson, T.S. Haddad, M.T. Bowers, Isomeric structural characterization of polyhedral oligomeric silsesquioxanes (POSS) with styryl and epoxy phenyl capping agents, Nano Lett. 4 (2004) 779–785.

[29] E.S. Baker, S.L. Bernstein, M.T. Bowers, Structural characterization of G-quadruplexes in deoxyguanosine clusters using ion mobility mass spectrometry, J. Am. Soc. Mass Spectrom. 16 (2005) 989–997.
[30] E.S. Baker, J.E. Bushnell, S.R. Wecksler, M.D. Lim, M.J. Manard, N.F. Dupuis, P.C. Ford, M.T. Bowers, Probing shapes of bichromophoric metal-organic complexes using ion mobility mass spectrometry, J. Am. Chem. Soc. 127 (2005) 18222–18228.
[31] A. Baumketner, S.L. Bernstein, T. Wyttenbach, G. Bitan, D.B. Teplow, M.T. Bowers, J.-E. Shea, Amyloid β-protein monomer structure: a computational and experimental study, Protein Sci. 15 (2006) 420–428.
[32] V. Gabelica, E.S. Baker, M.-P. Teulade-Fichou, E. De Pauw, M.T. Bowers, Stabilization and structure of telomeric and c-myc region intramolecular G-quadruplexes: the role of central cations and small planar ligands, J. Am. Chem. Soc. 129 (2007) 895–904.
[33] R. Bakhtiar, Mass spectrometric characterization of silsesquioxanes, Rapid Commun. Mass Spectrom. 13 (1999) 87–89.
[34] R. Bakhtiar, F.J. Feher, Mass spectrometric characterization of polyhedral oligosilsesquioxanes and heterosilsesquioxanes, Rapid Commun. Mass Spectrom. 13 (1999) 687–694.
[35] A.R. Bassindale, M. Pourny, P.G. Taylor, M.B. Hursthouse, M.E. Light, Fluoride-ion encapsulation within a silsesquioxane cage, Angew. Chem., International Edition 42 (2003) 3488–3490.
[36] A.R. Bassindale, D.J. Parker, M. Pourny, P.G. Taylor, P.N. Horton, M.B. Hursthouse, Fluoride ion entrapment in octasilsesquioxane cages as models for ion entrapment in zeolites. Further examples, X-ray crystal structure studies, and investigations into how and why they may be formed, Organomet 23 (2004) 4400–4405.
[37] S.E. Anderson, D.J. Bodzin, T.S. Haddad, J.A. Boatz, J.M. Mabry, C. Mitchell, M.T. Bowers, Structural investigation of encapsulated fluoride in polyhedral oligomeric silsesquioxane cages using ion mobility mass spectrometry and molecular mechanics, Chem. Mater. 20 (2008) 4299–4309.
[38] A. Somogyi, E.H. Elandaloussi, D.E. Hall, A. Buyle Padias, R.B. Bates, H.K. Hall Jr., Powerfully solvating matrices for MALDI-TOF spectroscopy of aromatic polyesters, Macromolecules 40 (2007) 5311–5321.
[39] J. Pyun, K. Matyjaszewski, Synthesis of hybrid polymers using atom transfer radical polymerization: homopolymers and block copolymers from polyhedral oligomeric silsesquioxane monomers, Macromolecules 33 (2000) 217–220.
[40] F. Lecolley, C. Waterson, A.J. Carmichael, G. Mantovani, S. Harrisson, H. Chappell, A. Limer, P. Williams, K. Ohno, D.M. Haddleton, Synthesis of functional polymers by living radical polymerization, J. Mater. Chem. 13 (2003) 2689–2695.
[41] D. Suckau, A. Resemann, M. Schuerenberg, P. Hufnagel, J. Franzen, A. Holle, A novel MALDI LIFT-TOF/TOF mass spectrometer for proteomics, Anal. Bioanal. Chem. 376 (2003) 952–965.
[42] A.S. Galhena, S. Dagan, C.M. Jones, R.L. Beardsley, V.H. Wysocki, Surface-induced dissociation of peptides and protein complexes in a quadrupole/time-of-flight mass spectrometer, Anal. Chem. 80 (2008) 1425–1436.
[43] A. Somogyi, P. Shu, A.B. Padias, D.E. Hall, H.K. Hall, Jr. "MALDI-TOF Analysis of Polymers by Using Tailor-Made Fluorinated Azobenzene and Stilbene Matrices", Presented at 55th ASMS Conference on Mass Spectrometry and Allied Topics, Indianapolis, IN, 2007.